Energy & Buildings 349 (2025) 116531

Contents lists available at ScienceDirect

Energy & Buildings

journal homepage: www.elsevier.com/locate/enb

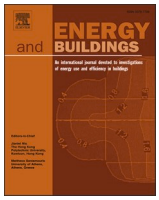

Experimental evaluation of radiant ceiling panels in office building perimeter zones

Hung Q. Do [a], Mark B. Luther [b], Jane Matthews [a,*], Igor Martek [a]

[a] School of Architecture and Built Environment, Deakin University, Geelong, VIC 3220, Australia
[b] Environmental Energy Services Pty. Ltd, Moolap VIC 3224, Australia

ARTICLE INFO

Keywords:
Radiant panels
Radiant cooling
Radiant heating
Thermal comfort
Perimeter zone

ABSTRACT

Lightweight and modular radiant ceiling panels are attracting increasing interest from researchers, project owners, and designers. However, their thermal performance and capacity to deliver comfort in perimeter office zones remain underexplored. This study evaluates the performance of a prototype lightweight radiant ceiling panel system in a test chamber constructed in Victoria, Australia, to emulate a north-facing perimeter office space. The system, designed for both heating and cooling, was assessed through two cooling test runs and one heating test run. Results show that the panels are highly responsive, thermally effective, and capable of maintaining thermal comfort, particularly under cooling conditions. The system achieved average capacities of 95 W/m^2 in cooling and 85 W/m^2 in heating. In cooling mode, it successfully countered perimeter solar heat gains while maintaining appropriate comfort levels. Heating, though viable, responded more slowly and produced significant vertical air temperature gradients, potentially causing local discomfort. To mitigate this, supplementary mechanical ventilation is recommended. While broadly consistent with prior research, the study highlights the need for at least three test runs in both heating and cooling to improve generalizability. Future experiments with an upgraded heat pump and improved storage tank are planned to validate and extend these findings.

1. Introduction

Perimeter zones in office buildings are the most problematic areas due to heavy exposure to the external environment [1]. Among the external elements that affect the thermal condition of perimeter zones, solar heat gain and heat exchanges through glazing windows are the most significant [2]. Most of the solutions to counter the heavy heat exchange at the perimeter zones focus on enhancing the envelope [2] and intensifying the conditioning capacity at perimeter zones [3,4]. However, increasing conditioning capacity at perimeter zones with conventional convective systems can be highly energy-intensive [5]. Instead, radiant conditioning systems have emerged to be a thermally effective and energy-efficient alternative [6].

Meanwhile, radiant conditioning systems, especially radiant ceilings, have gained popularity among designers and researchers. The main reason may rest in the convenient application of radiant ceiling systems. Unlike other types of radiant systems that are mostly limited to being used in new projects, radiant ceilings can be used for both retrofitting existing buildings and new projects alike [6].

Several studies have focused on evaluating the performance of radiant ceiling systems. This includes focusing on enhancing the design of panels to maximise heat transfer. For example, Zhang *et al.* [9] conducted an instrumental experiment to evaluate a new radiant cooling ceiling design with inclined fins. In this study, the authors focus on enhancing heat transfer between the radiant ceiling and the conditioned environment via promoting convection. Although the system was tested in two perimeter zones, the testing did not include the impact of direct solar radiation, potentially the most influential external factor in perimeter zones.

While some studies have focused on the impact of direct solar radiation, their evaluation has largely concentrated on the cooling load. For example, Feng *et al.* [7] used simulation to compare the cooling load between a radiant ceiling and a convective system. The authors tested different types of radiant systems under the same conditions, notably impractical in full-scale experiments. The results show that at the perimeter zone with direct solar heat gain, the peak cooling load for the

* Corresponding author.
E-mail addresses: qhdo@deakin.edu.au (H.Q. Do), mark.b.luther@gmail.com (M.B. Luther), jane.matthews@deakin.edu.au (J. Matthews), igor.martek@deakin.edu.au (I. Martek).

https://doi.org/10.1016/j.enbuild.2025.116531
Received 22 January 2025; Received in revised form 28 September 2025; Accepted 29 September 2025
Available online 30 September 2025

radiant system can be significantly higher than that of the convective system, up to 49 % for the TABS (thermal active building system) radiant ceiling. Also, reducing direct solar radiation using shading systems results in a lower peak load for radiant cooling ceilings. With a similar goal, but instead through an instrumental experiment, Moftakhari *et al.* [8] compared the performance of radiant and convective systems at perimeter zones. Here, the relationship between solar heat gain and the thermal performance of radiant systems is again investigated in terms of the internal conditioning load. The radiant ceiling is shown to be more effective than the convective system in absorbing heat from solar radiation. Again, a higher peak cooling load is recorded for the radiant ceiling at the perimeter zone, reinforcing that direct solar heat gain has a notable impact on the performance of radiant ceiling systems. While the comparison of conditioning loads is important in evaluating the performance of radiant ceiling systems at perimeter zones, there have been notably few studies conducted to evaluate their capability to provide thermal comfort, which ultimately is the fundamental aim of such systems.

Where examples of comfort evaluation exist, the window-to-wall ratio is typically low. Jia *et al.* [6], for instance, conducted an experiment to study the performance of radiant ceiling and floor systems in an office space located in California, USA, including thermal comfort. While they concluded that their system was capable of providing thermal comfort, unfortunately, their testing facility could not support evaluation of window-to-wall ratios above 50 %.

In evaluating the capability of radiant systems in general to provide thermal comfort, Fanger's model, commonly known as Predicted Mean Vote (PMV) or Predicted Percentage of Dissatisfied (PPD), is commonly used. For example, PMV is used in the simulation studies of Ding *et al.* [10] to evaluate the performance of different radiant fin ceiling designs. PMV is also the key parameter to evaluate the radiant ceiling panels in a sleeping environment in the simulation study of Du *et al.* [11]. In their experimental and simulation study, Miriel *et al.* [12] used PPD to measure the capability to provide thermal comfort of radiant heating and cooling ceiling at a perimeter zone subject to solar heat gain. The results show that while a heated ceiling can provide adequate thermal comfort, the capability to provide thermal comfort during cooling can be limited when subject to heavy solar heat gain. Similarly, in the study of Serageldin *et al.* [13], a radiant cooling ceiling system with segmented concave surfaces is evaluated using PMV in a perimeter zone. In this experimental study, the results indicate that the concave surface can provide more favorable thermal comfort conditions than conventional flat ceilings, although, notably, no analysis on the impact of solar heat gain was conducted. Zhao *et al.* [14] also used PMV to evaluate their radiant system which consisted of an exposed capillary ceiling powered by a solar water heater and an air-source heat pump. Their radiant ceiling is tested in heating mode with four different supply water temperatures. The result shows that the heating ceiling cannot provide thermal comfort if the supply water is about 30 °C but when the supply water is about 35, 39.7, or 45.5 °C, thermal comfort is successfully achieved.

While some progress has been made in evaluating the potential of radiant ceilings at perimeter zones, the relationship between the external environment, especially solar heat gain, the ceiling's thermal performance, and the thermal comfort level achieved has received little attention. Therefore, this study aims to investigate the thermal performance, including the capability of providing thermal comfort, of a radiant conditioning ceiling in a perimeter zone, both in cooling and heating. In order to realistically evaluate the capability to provide thermal comfort, our newly developed radiant ceiling panels are tested in a full-scale experiment with a window-to-wall ratio up to 70 %.

The contributions of this study are therefore threefold:

- The evaluation of two new panel designs, configured in a ceiling system to match the conditioning demands of perimeter zones. The panels are developed to be lightweight, easy to produce and install, and high-performing.
- The instrumental measurement of the capability of the radiant ceiling system to provide and maintain thermal comfort in both heating and cooling modes.
- In cooling mode, the high-window-to-wall ratio experimental test space is subjected to high solar gain to fully emulate the problematic conditions of a perimeter zone and realistically evaluate the system's capability in terms of thermal comfort.

Hence, this study not only focuses on the measurement of radiant ceiling thermal performance variables such as heat flux or panel surface temperature, but also investigates comfort-related variables such as temperature stratification, mean radiant temperature (MRT), and PMV. Furthermore, external variables such as transmitted solar radiation and external temperature are critical in this study. In addition, our radiant ceiling is tested as the primary system, not as a supplement to convective (HVAC) systems. Therefore, this study allows us to evaluate the limits of radiant conditioning when considering variables such as solar heat gain and external temperature.

2. Methodology and data collection

2.1. Research design

This study aims to evaluate the thermal performance of a lightweight radiant ceiling panel system and its capability to provide thermal comfort in perimeter zones in office buildings. In particular, this study seeks to better understand the limits of radiant conditioning ceilings in obtaining a suitable comfort level in perimeter zones in office buildings.

A full-scale empirical study is conducted to better understand the impact of external environmental inputs. The experiments are conducted within a test chamber (Test-Cell) purposely built to emulate the conditions of a north-facing perimeter room in an office building. Note, the experiments are conducted in the southern hemisphere, hence the north-facing façade receives the most direct solar radiation. Similar approaches have been commonly used in previous studies. For example, to evaluate a dual heat source radiant ceiling system, Zhao *et al.* [14] conducted a similar full-scale instrumental experiment in a test chamber. However, the radiant ceiling tested is without the finishing, and the capillary tubes are exposed to the internal environment. Similarly, Joe and Karava [15] conducted a full-scale experiment in three perimeter office rooms to evaluate their control strategy for the high thermal mass radiant floor. In this study, we additionally focus on investigating PMV and solar heat gain.

2.2. The test chamber (Test-cell)

To provide an environment for full-scale experimental evaluation, an experimental "Test-Cell" is constructed in compliance with Australian standards. The Test-cell is built inside an industrial shed to mimic an office room in a larger office building. The Test-cell floor, ceiling, and 3 walls (south, east, and west) are within the shed interior; the north-facing wall can be opened to the external environment via a sliding gate. The Test-cell is 3 m high, 4.8 m deep, and 3.6 m wide with a north-facing, fixed, double-glazing window (Fig. 1). The window is 3 m wide and 2.4 m high (about 7.5 m^2 of north-facing glazing). Hence, the north-facing window-to-wall ratio is about 70 %. A perimeter zone is often considered to be 3–5 m deep in the floor plan; hence, the Test-cell size is adequate. An external sliding gate can be used to adjust the exposure of the window to direct solar radiation. The Test-Cell is built with a metal stud frame and insulated with earth wool, complying with the Australian National Construction Code.

The ceiling in the Test-Cell is 3.6 × 4.8 m and was built with a commonly used Australian suspended ceiling system comprising 1.2 × 0.6 m tiles (24 tiles). Fig. 2 shows the ceiling arrangement. In this study,

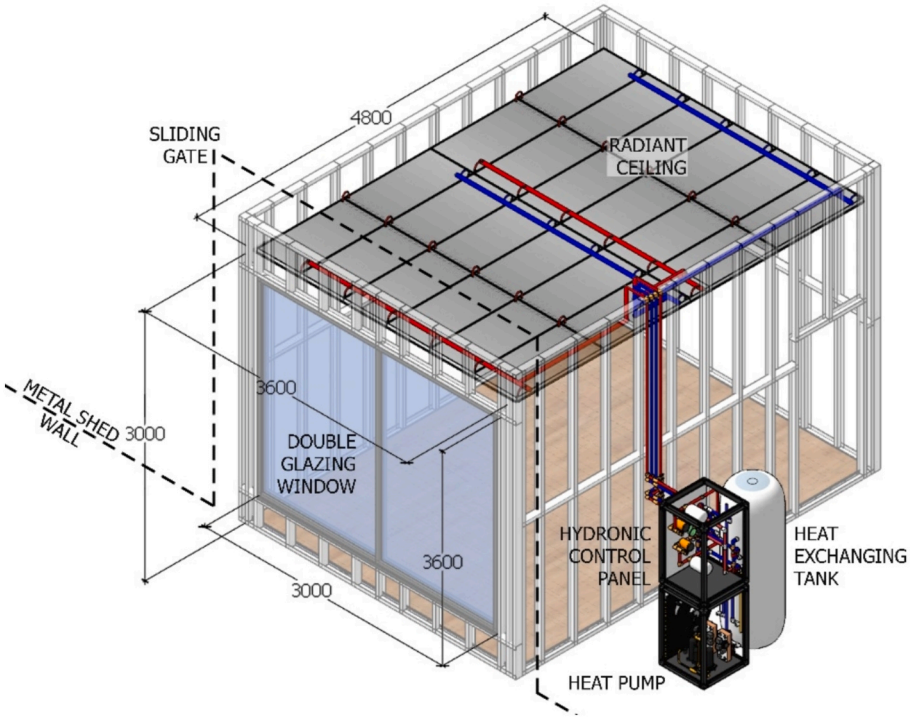

Fig. 1. Test-Cell diagram.

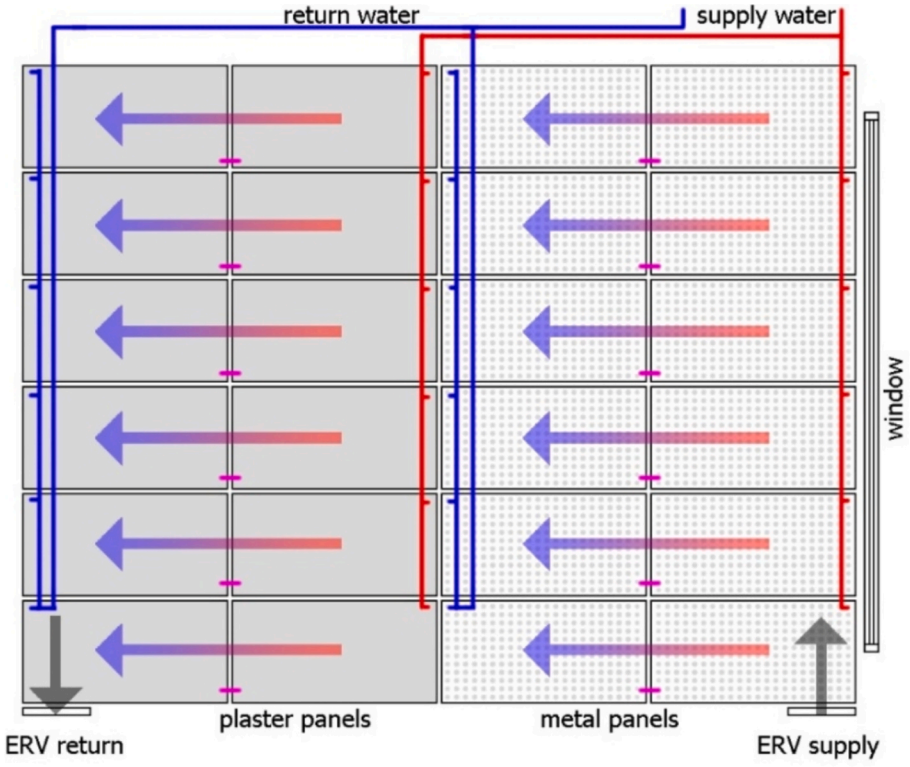

Fig. 2. Radiant Ceiling Diagram.

all of the 24 ceiling tiles are radiant conditioning panels developed based on the results of our previous research [16]. The panels are paired together in series; thus, the water goes through one panel before entering the other. Six pairs are connected in parallel in a group of 12.

Each group of radiant panels has a supply water and a return water manifold. The main supply and return manifold pipes are arranged so that the flow channel in a panel group is "canopy to canopy," which is recommended by Mosa *et al.* [17] to ensure equal water flow throughout the ceiling. The conditioned water is supplied from the nearest points to the window and flows toward the back wall.

The purpose of supplying conditioned water to the panels near the window first is to intensify the conditioning effect near the window,

where external conditions show their effect the most. In conditioning perimeter zones, intensifying the conditioning capacity with extra conditioning systems near the windows is the preferred method [18]. Intensifying the radiant system near the window is also recommended by the REHVA handbook [19] for radiant concrete floors and is practiced by our industrial partners and radiant systems installers, yet not discussed in research publications.

For mechanical ventilation, the Test-Cell is equipped with an energy-recovering ventilation system (ERV). The return duct terminal is located near the back wall, while the supply terminal is next to the window (Fig. 2). The heat-recovering system can add air movement (air velocity) to the Test-Cell while ensuring that the convective heat transfer between the Test-Cell and the external environment is minimized.

2.3. Radiant panels

The radiant ceiling consists of a series of prefabricated, modular, and lightweight hydronic panels. As shown in Fig. 2, there are two types of radiant panels used in the ceiling. Both of the two designs are classified by the REHVA handbook for radiant systems as a variant of 'Type B' Embedded Surface Systems (ESS) [19]. They have similar designs, with the only difference being the material of the radiant surface (finishing surface). The 12 panels (half of the ceiling) closest to the window use perforated metal ceiling tiles as radiant surfaces (metal panels) while the remainder of the panels, towards the rear of the cell, use plasterboard ceiling tiles (plaster panels). The panel designs are shown in Fig. 3.

The radiant surface (finishing surface) of the "metal panel" is a 1200x600mm perforated metal ceiling tile, and a 6 mm thick 1200x600mm plasterboard-based ceiling tile is used for the "plaster panels". Designing a radiant panel based on Australian commonly used ceiling tile dimensions allows the non-thermally active ceiling tiles to be replaced by thermally active panels without affecting the accepted architectural appeal. While the plasterboard-based ceiling tile is commonly used in commercial and office buildings in Australia and is widely available on the market at reasonable prices, the perforated metal ceiling tiles are expensive, with limited supply. In radiant panel designs, the lower thermal mass (only 1 kg) and thermal resistance of the perforated metal ceiling tiles promise better thermal performance [16]. Hence, the "plaster panels" are considered to be the affordable option, while the metal panels are considered premium. The superior, but more expensive, metal radiant panels are placed near the window. The purpose of such an arrangement is to intensify the conditioning capacity near the window, as suggested by the REHVA handbook. Both the "plaster panels" and the "metal panels" were designed based on the lessons learned from two previous studies (Do *et al.*[16] and Do *et al.* [20]).

All of the panels used plastic capillary tube mats for a more uniform surface temperature and higher heat transfer [21,22]. The flow channel used for the capillary tube mat is the "canopy to canopy" flow channel proposed by Mosa *et al.* [17] for fast and even distribution of water through the panels. The metal pans are designed to "warp" around the capillary tube and are used as a heat-conducting as well as distributing element of the panels, ensuring an effective heat transfer connection and balanced heat distribution. In type B ESS, the capillary tube and the metal pans are embedded in the insulation layer at the back of the panels.

Also, in radiant panel design, contact thermal resistance should be avoided [23]. Thus, the layered components of a panel are firmly glued together to eliminate thermal contact resistance. In our previous design science research, the full-contact adhesive full contact method in building results in enhanced thermal performance for radiant panels. Plus, this method increases the panels' structural durability, as well as forming a completed prefabricated product.

2.4. Equipment, sensors, and experiment setup

The instruments and sensors used in this study include two thermal comfort carts, four heat flux sensors with built-in thermocouples, 6 thermocouples, a thermal imaging camera, a weather station with two additional pyranometers, and a digital flow rate sensor on the pump side.

A thermal comfort cart is a field study instrument consisting of a series of sensors, including air velocity, air temperature, air humidity, black globe temperature, and CO2 sensors. De Dear and Brager [24] and

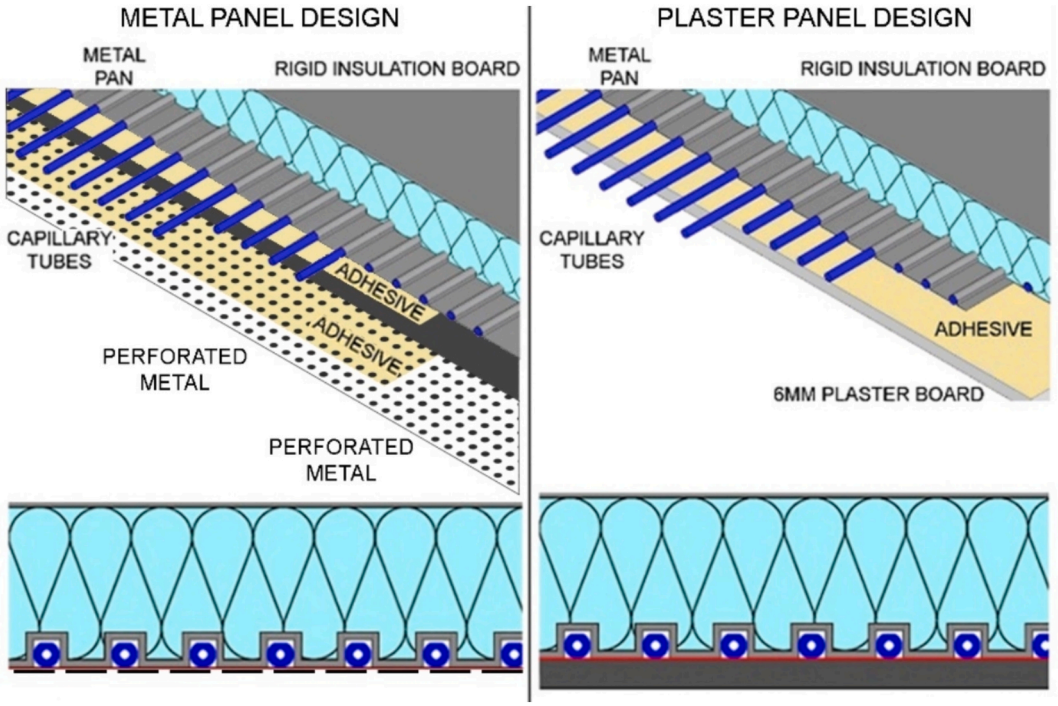

Fig. 3. Ceiling panel designs.

Luther *et al.* [25] utilized similar instruments to determine the level of thermal comfort in their study. The instrument complies with the ASHRAE 55 standard of thermal comfort. On the thermal comfort cart, there are 3 sets of sensors. Each set includes an air velocity sensor, an air temperature sensor, an air humidity sensor, and a black globe temperature sensor. The sensor sets are located at 0.1 m, 0.6 m, and 1.1 m above the ground, equivalent to the height of the feed, body, and head of a sitting person, respectively. This setup allows the thermal comfort level (PMV) can be calculated at different body parts of a sitting person and to analyze local discomfort. An additional air temperature sensor and an air velocity sensor are located at 1.5 m high above the ground (standing person's head height). Thus, the thermal comfort carts can also measure air temperature stratification up to 1.5 m high.

The sensors are connected and collected using a Campbell Scientific CR32X data logger board. The data collected by the comfort cart can then be used to calculate the mean radiant temperature (MRT), operative temperature (OT_a), and thermal comfort predicted mean vote (PMV). Two thermal comfort carts are used in this study. Comfort cart 1 (CC1) is placed near the window, while comfort cart 2 (CC2) is placed near the back wall. Note that it is important not to have solar radiation directly on the black globe temperature sensors and other sensors, since the reading will not be valid for use.

The experiment setup is shown in Fig. 4. The water supplied to the ceiling is conditioned using a heat pump and stored in a tank with a heat exchanger. At the hydronic control panel, the temperature of the conditioned water is regulated, and the water is pumped to the ceiling. Four FHF05 heat flux foil sensors with built-in thermocouples are applied at the center of the panels across the ceiling to monitor their thermal performance. All four heat flux sensors are certified and calibrated prior to installation. Additional thermocouples are applied to the supply and return water pipes to monitor the inlet and outlet water temperatures.

As the perimeter zones are highly affected by external weather conditions, a weather station is used to monitor the external environment. In the case of this study, the required variations are the global solar irradiance (horizontal) and the external air temperature. Two solar irradiance sensors (pyranometers) are used to monitor the solar gain of the chamber. The pyranometers are placed vertically, parallel with the north-facing façade and window. One pyranometer is located outside of the Test-cell, mounted directly on the façade for monitoring the solar gain received by the façade. The other pyranometer is located behind the double-glazing window, monitoring the solar radiation transmitted through the glazing and entering the Test-cell through the window glazing, thus monitoring the solar heat gain of the Test-cell interior. The readings from the weather station and the two pyranometers are collected with a CR1000 data logger board.

In addition, a thermal imaging camera is also used to aid the monitoring process, such as finding representative spots to apply sensors, troubleshooting, or cross-checking with sensor readings. At the hydronic control panel, there is a digital flow meter used to monitor the water flow rate.

2.5. Experiment principle

The experimental evaluation is conducted in two conditioning modes, heating and cooling. In both cases, the radiant ceiling is the only conditioning device. Additional ventilation and air movement can be (or not) provided through an energy-recovering ventilation system (ERV); this is the only intervention made other than the radiant ceiling itself. Therefore, this study is absent of any other conditioning that would normally occur from an HVAC system in this zone. It is noted that convective air conditioning could dramatically improve any negative comfort result from radiant conditioning alone.

In the heating mode experiment, a single test run (Test 1) is conducted in cold weather (below 16 °C air temperature) and with the gate closed. This ensures that the chamber receives no extra solar heat gain, and the only heat source the Test-cell has is the heating ceiling. The heating inlet water temperature is set at 40 °C with the water flow rate supplied to the whole ceiling at about 11 L/min (more than 60 changes per hour). Two additional preliminary heating test runs were conducted to test the functionality of the instrumentation and the system, prior to Test 1.

Two experiment test runs (Test 2 and Test 3) are conducted in cooling mode. In Test 2, the cooling ceiling has to overcome the solar heat gain from a 7.5 m^2 north-facing glazed window (70 % window-to-wall ratio) on a sunny day without aids from external shading or mechanical ventilation. However, in normal operation of a realistic office building, on hot sunny days, when the building receives heavy solar radiation, shading systems and extra ventilation will be applied as a norm to counter solar heat gain. Hence, in Test 3, the cooling ceiling works in conjunction with an energy-recovering ventilation (ERV) system and an external shading system. The external shading is emulated by partly closing the north-facing gate. During Test 3, the proportion of the window exposed to direct sunlight is 50 % (about 3.7 m^2). The

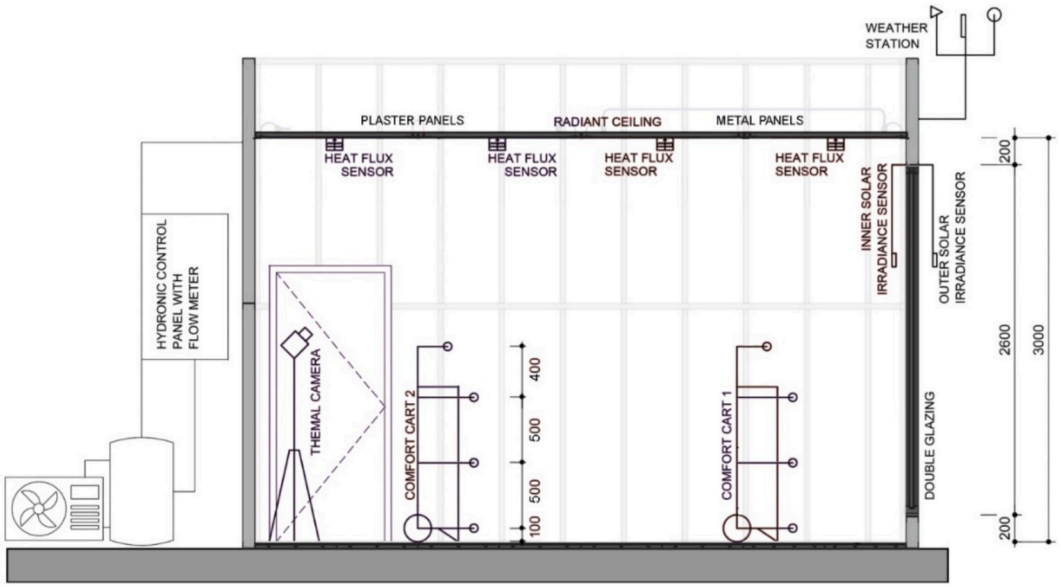

Fig. 4. Experiment setup.

cooled water is supplied to the ceiling at the rate of about 10 L/min (more than 55 changes per hour). Preliminary cooling test runs were also conducted to calibrate the instrumentation and confirm the functionality of the system, prior to Test 2 and Test 3. The test runs are summarized in Table 1.

Each test run lasts about three to four hours. The conditioning water (hot or cold) is prepared prior to the test runs. During the test run, the system is fully operational with the heat pump running. The high flow rate of about 9 to 11 L/min ensures a fast and constant flow of water throughout the ceiling. After a test run, the system is turned off, and the supply of conditioned water to the ceiling is cut, and the room is left to "cool down". The data recording commenced at least one hour before the test run and concluded at least one hour after, ensuring that the conditions before, during, and after the test runs are recorded.

2.6. Parameters to be measured and calculated

Table 2 shows the parameters measured or calculated in this study. PMV and PPD are calculated based on the ASHRAE standard 55 [26], shown in Fig. 5. The variables required for the PMV calculation include air temperature (Ta), relative humidity (Rh), air velocity (v), mean radiant temperature (MRT), metabolic rate (Met), and level of clothing (Clo), and are primarily collected via the two thermal comfort carts positioned within the Test-Cell. The resulting PMV from the two comfort carts is subsequently averaged for a representative PMV level of the Test-Cell. Additionally, comparing the readings from the two carts gives a more detailed view of the Test-cell conditions.

Among the variables, air temperature, air velocity, and air humidity are directly measured by the comfort carts. The Mean Radiant Temperature (MRT) is calculated based on air temperature, air velocity, and the black globe temperature, which are directly measured by the comfort carts. Following the ASHRAE standard 55, MRT is calculated according to the equation below:

$$T_r = \{(T_g + 459.67)^4 + [V_a^6 \times 4.74 \times 10^7 \times (T_g\text{-}T_a)] / (D^4 \times 0.95)\}^{0.25} - 459.67 \quad (1)$$

Where:

T_r is the mean radiant temperature (°C or K).

T_g is the black globe temperature (°C or K).

T_a is the air temperature (°C or K).

D is the diameter of the black globe (mm).

The black globes used in the thermal comfort carts are 36 mm in diameter.

The clothing level and metabolic rate are determined based on the ASHRAE standard 55 (Fig. 5). Here, the metabolic rate for an office working condition is approximately 1.1, the indoor winter closing level (Heating session) is 0.9, and for summer (Cooling session) is 0.6. Hence, the metabolic rate of 1.1 is used in all PMV calculations. While the closing level of 0.9 is used in a heating test run, the closing level of 0.6 is used in cooling experiments.

Based on the ASHRAE Standard 55 (Fig. 5), PMV and equivalent thermal sensation are shown in Table 3 below:

As the main purpose of this study is to evaluate the capability of the radiant ceiling to provide thermal comfort, the most crucial parameter to be analyzed is PMV. While the ASHRAE 55 standard states PMV values ranging from −0.5 to 0.5 (10 % PPD or 90 % satisfied) are optimal [26], such a high level of thermal comfort can be considered hard to achieve, and energy-intensive [26] and conservative [25]. Instead, the range from −0.8 to 0.8 (20 % PPD or 80 % satisfied) is recommended as acceptable [25,26] and will be adopted in this study.

Another crucial variable in evaluating thermal comfort is Operative temperature (T_o). Operative temperature is considered the closest representation of human temperature sensation [27]. Additionally, in an environment with controlled airspeed, the operative temperature should closely follow the PMV values [26]. To evaluate the effect of radiant conditioning, the air temperature, MRT, and operative temperature will be compared. Operative temperature is calculated based on ASHRAE 55 (Eq. 2).

$$To = A*Ta + (1\text{-}A)\text{–}Tr \quad (2)$$

Here, A is the coefficient value based on the air velocity (V_a). If the air velocity is lower than 0.2 m/s, then $A = 0.5$; if the air velocity is between 0.2 to 0.6 m/s, then $A = 0.6$; and if the air velocity is higher than 0.7 m/s, then $A = 0.7$.

The calculated operative temperature is also vital in evaluating the thermal performance of radiant systems. Here, the total heat transfer

Table 1
The test runs are summarized.

Test run	Conditioning mode	Window exposure	Ventilation	Inlet water temperature set point	Flow rate
Test 1	Heating	0 m^2 (closed)	None	37 °C	11 L/min
Test 2	Cooling	7.5 m^2 (100 %)	None	12 °C	10 L/min
Test 3	Cooling	3.7 m^2 (50 %)	EAV (150 m^3/hr)	12 °C	10 L/min

Table 2
Variables measured or calculated.

Variable	Symbols	Unit	Collection
Air temperature	T_a	°C or K	Thermocouple
Radiant surface (ceiling) temperature	T_s	°C or K	Thermocouple
Mean radiant temperature	T_r	°C or K	Calculation
Black globe temperature	T_g	°C or K	Thermal comfort cart
Relative Humidity	R_h	%	Thermal comfort cart
Heat flux (heat transfer)	q	W/m^2	Heat flux sensor
Heat transfer coefficient	H_t	W/m^2K	Calculation
Air velocity	V_a	m/s	Thermal comfort cart
Operative temperature	T_o	°C or K	Calculation
Inlet water temperature	T_w	°C or K	Thermocouple
Water flowrate	f	L/min	Flowmeter
Thermal comfort (PMV)	PMV		Calculation
Solar irradiant	Q_{sl}	W/m^2	Pyranometer
External air temperature	T_{ex}	°C or K	Weather station

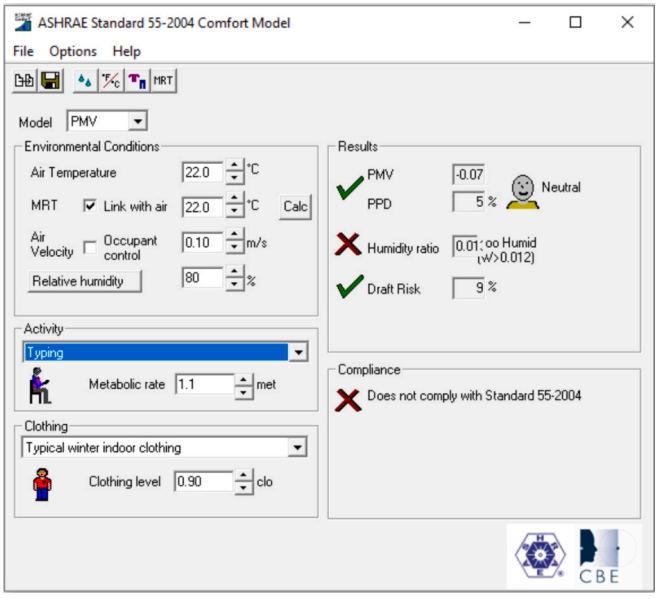

Fig. 5. ASHRAE Standard 55 comfort model (PMV).

Table 3
PMV and equivalent thermal sensation.

PMV	−3	−2.5	−2	−1.5	−1	−0.5	0	0.5	1	1.5	2	2.5	3
Thermal Sensation	Hot	Warm		Slightly Warm		Neutral		Slightly Cool		Cool		Cold	

between the radiant system and the conditioned environment is the result of the difference between the radiant surface temperature of the ceiling and the operative temperature of the conditioned environment [28]. The relationship between the radiant ceiling heat flux, operative temperature, and radiant ceiling surface temperature is shown in the equation below.

$$q = h_t(T_o - T_S) \quad (3)$$

Where:
q is the total heat flux (W/m^2).
h_t is the total heat transfer coefficient (W/m^{2}K).
T_o is the ambient operative temperature (°C or K).
T_s is the radiant surface temperature (°C or K).

In a conventional working environment, there are two heat transfer mechanisms between the radiant system and the conditioned environment, namely convective and radiative [19]. Accordingly, the total heat transfer coefficient consisted of the radiant and convective heat transfer coefficients:

$$h_t = h_c + h_r \quad (4)$$

Where:
h_c is the convective heat transfer coefficient (W/m^{2}K).
hr is the radiant heat transfer coefficient (W/m^{2}K).

In the conventional operation of radiant conditioning systems, the radiant heat transfer coefficient is 5.5 W/m^{2}K [28].

The operation of the ceiling is indicated by the heat transfer between the ceiling and the room, the surface temperature, and the inlet water temperature. The readings of the four heat flux sensors are averaged. The same procedure is also applied to the panel surface temperature. The air stratification can also indicate the operation of the ceiling and how different conditioning modes affect convective heat transfer. Here, we focus only on the stratification between the floor and the standing head height (1.5 m above the floor).

In cooling mode experiments, as the Test-cell is unoccupied, the heat gain is mainly solar. The transmitted solar radiation provides for solar heat gain to be calculated and compared with the total cooling capacity of the ceiling.

3. Experiment results

This section provides the results of the three test runs and provides initial brief discussions.

3.1. Radiant heating ceiling (Test 1)

In Test 1, the radiant ceiling is operated in heating mode.

Thermal comfort and ceiling operation

Fig. 6 shows the results of the heating test run, including the ceiling average temperature (average radiant surface temperature – T_s), thermal comfort level (PMV), mean radiant temperature (MRT- T_r), and operative temperature (T_o). Overall, there is a clear connection between the calculated operative temperature (T_o) and PMV, as the two variables follow each other closely. Also, there are no notable differences between the Test-Cell temperatures, including average MRT (T_r), air temperature (T_a), and operative temperature (T_o). Before the heating ceiling is activated, the room's operative temperatures and the ceiling temperature are similar and stable at about 16 °C. As a consequence, the PMV is at uncomfortably cool levels of about −1.8 to −2 (cool).

As the heating ceiling is activated, the temperature of the ceiling (T_s) sharply rises to about 33 °C and remains stable around 32 to 34 °C during the heating session. This surface temperature complies with the recommendation of the REHVA handbook for heating the ceiling (35 °C

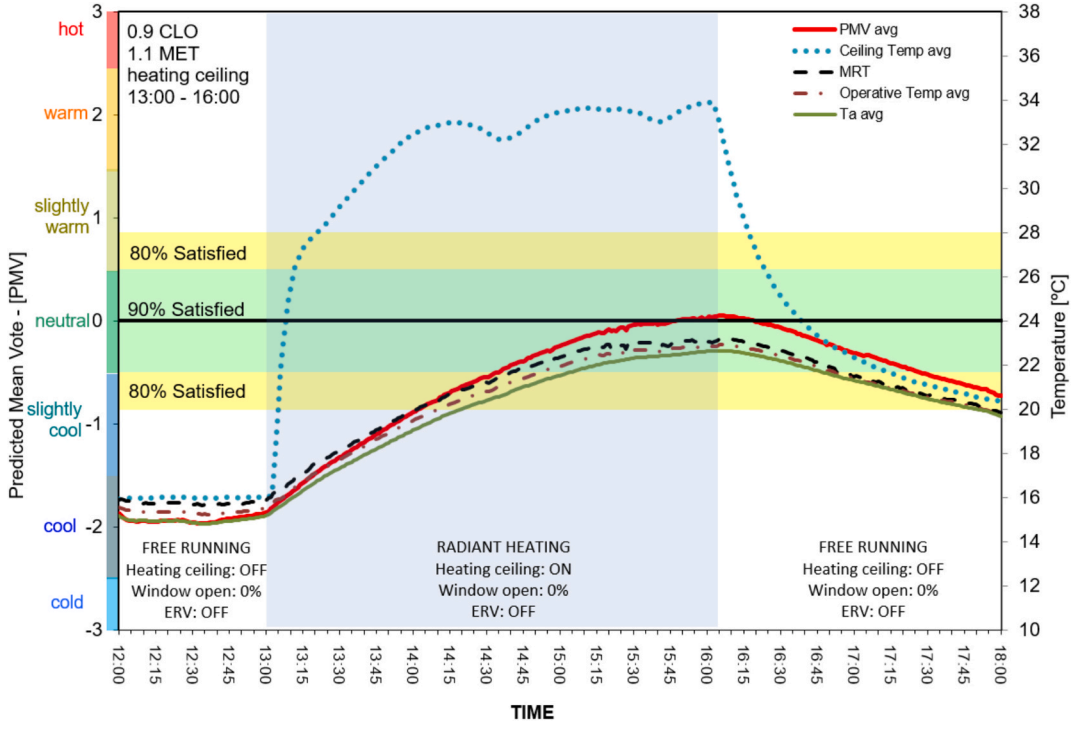

Fig. 6. Test 1 (Heating) – Thermal comfort, Ceiling Temperatures, MRT, and Operative Temperatures.

maximum). As a result, the PMV steadily increased from −2 (cool) and reached the optimal thermal comfort level of 0 (neutral). At this point, the heating session ceases, and the ceiling is left to "cool down" on its own.

As the hot water supply is terminated, the ceiling temperature (T_s) reduces from 34 °C to 20 °C in about 2 h. As a result, the Test-Cell cools and the PMV and the Test-Cell temperatures (T_o, T_r, T_a) reduce slowly, but steadily. Interestingly, even after the heating ceiling is deactivated, the condition within the test chamber remains thermally comfortable for about two hours.

Stratification

Fig. 7 shows the vertical temperature stratification of the test chamber. Prior to the heating session, there is a relatively uniform thermal condition within the Test-Cell. The air temperature (T_a) difference between the standing head height (1.5 m) and near the floor (0.1 m) is approximately 1 °C, and there are no significant temperature differences recorded between the two comfort carts. Yet, when activated, the heating ceiling starts to create stratification within the Test-Cell, with the temperature differences between heights increasing throughout the heating session. In particular, the closer to the ceiling, the higher the air temperature. At the end of the heating operation, the air temperature (T_a) difference between the 1.5 m high (standing head high) and 0.1 m high (near floor) can be up to 3 °C, as recorded by comfort cart 1 (CC1).

Ceiling thermal performance.

Fig. 8 shows the thermal performance of the heating ceiling. Prior to the test run, the ceiling temperature (T_s) is close to the Test-Cell operative temperature (T_o) at about 15 °C. As a result, the ceiling heat flux (q) readings are close to 0 W/m^2. There is almost no heat transfer between the ceiling and the inner environment of the Test-Cell. As the heating session starts, the inlet water temperature (T_w) quickly increases, reaching about 37 °C. As a result, the ceiling temperature (T_s) rises to about 33 °C. The heat flux (q) reading at the front zone reaches 85 W/m^2. Applying the readings to equation 3 (Eq. 3), the resulting heat transfer efficiency (h_t) is only about 6.3 W/m^{2}K during the heating session. Unfortunately, some fluctuations in inlet water temperature were experienced during the heating operation. These fluctuations were an unavoidable constraint of the heat pump operation.

3.2. Radiant cooling ceiling (Test 2)

In Test 2, the ceiling is run in cooling mode with the Test-Cell window fully open (7.5 m^2) and the ventilation system (ERV) is off.

Thermal comfort and ceiling operation

Fig. 9 shows the results of the second test run (radiant cooling ceiling), including thermal comfort level (PMV), operative temperatures (T_o), mean radiant temperature (MRT-T_r), and ceiling temperature (T_s). Once again, the PMV value follows the Test-Cell internal temperatures (T_a, T_r, T_o) closely with no significant differences between temperatures during the measurement.

At the start, the Test-Cell internal temperatures (T_a, T_r, T_o) are about 19 °C while the ceiling temperature (T_s) is about 21 °C. As the window is opened, the Test-Cell receives direct solar radiation and heats up quickly. The Test-Cell internal temperatures (T_a, T_r, T_o) rise sharply up to about 26 °C in 1.5 h. As a result, the PMV values also increased accordingly, from about −1.1 (slightly cool) to 0.75 (slightly warm). To maintain an acceptable level of PMV (below 0.8), the cooling ceiling is activated.

As the cooling ceiling is activated, the average temperature of the ceiling (T_s) drops sharply from about 26 °C down to about 15 °C in about 15 min and is maintained at about 16 °C throughout the session. The cooling ceiling shows an almost immediate effect, and the rising trend of the Test-Cell internal temperatures (T_a, T_r, T_o) and PMV is stopped. Instead, during the cooling session, the Test-Cell internal temperatures (T_a, T_r, T_o) decrease slightly from 26 °C to about 24 °C. Accordingly, the PMV at the front zone reduces from about 0.75 (slightly warm) down to 0.3 (neutral) and remains at this level during the cooling session.

As the cooling operation is concluded, the ceiling temperature (Ts) quickly rises to about 31 °C in 1.5 h. In the meantime, the Test-Cell internal temperatures (T_a, T_r, T_o) rise 5 °C to about 29 °C, resulting in

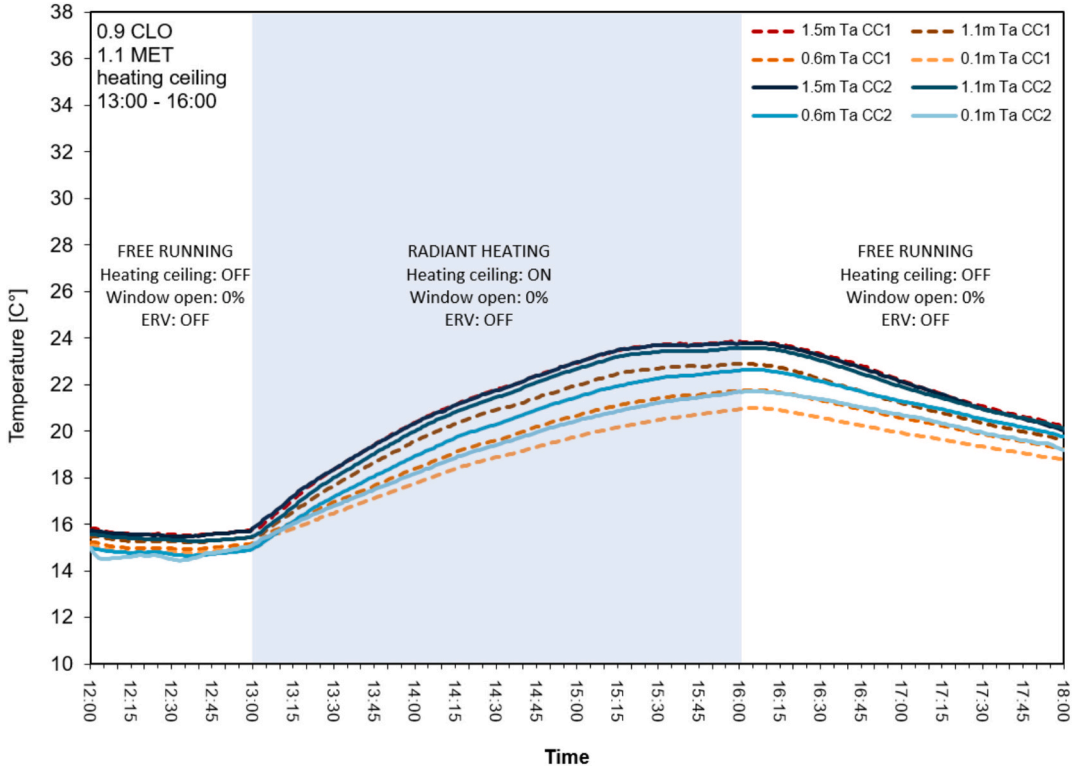

Fig. 7. Test 1 (Heating) – Temperature Stratification.

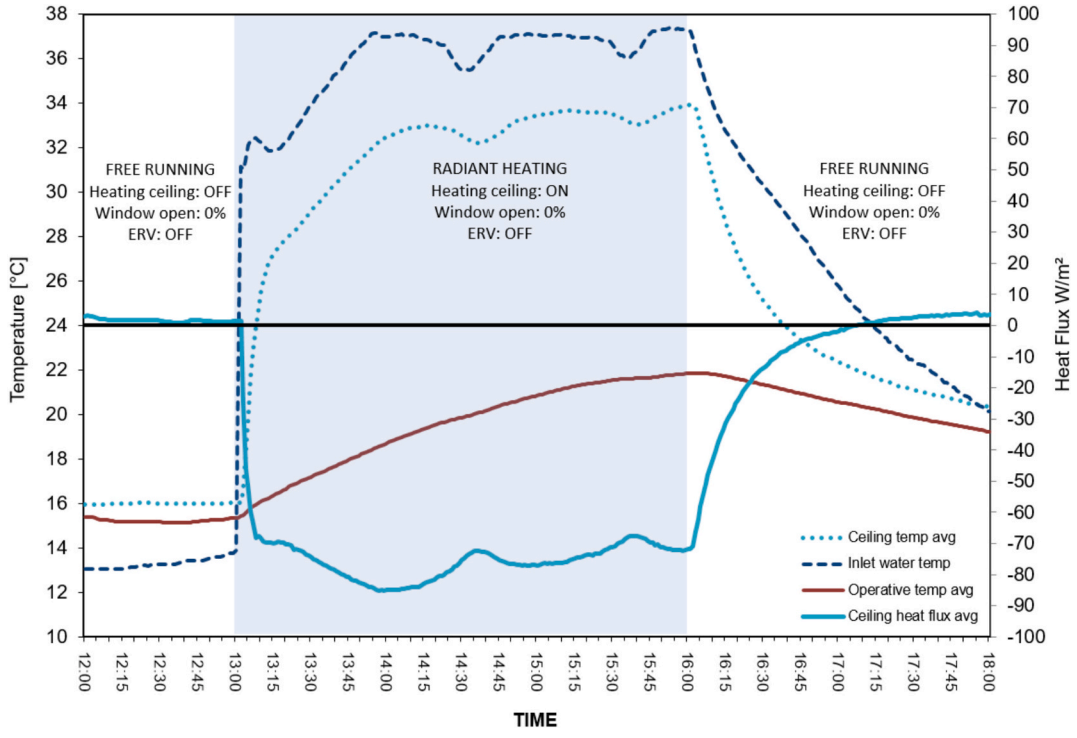

Fig. 8. Test 1 (Heating) – Ceiling Thermal Performance.

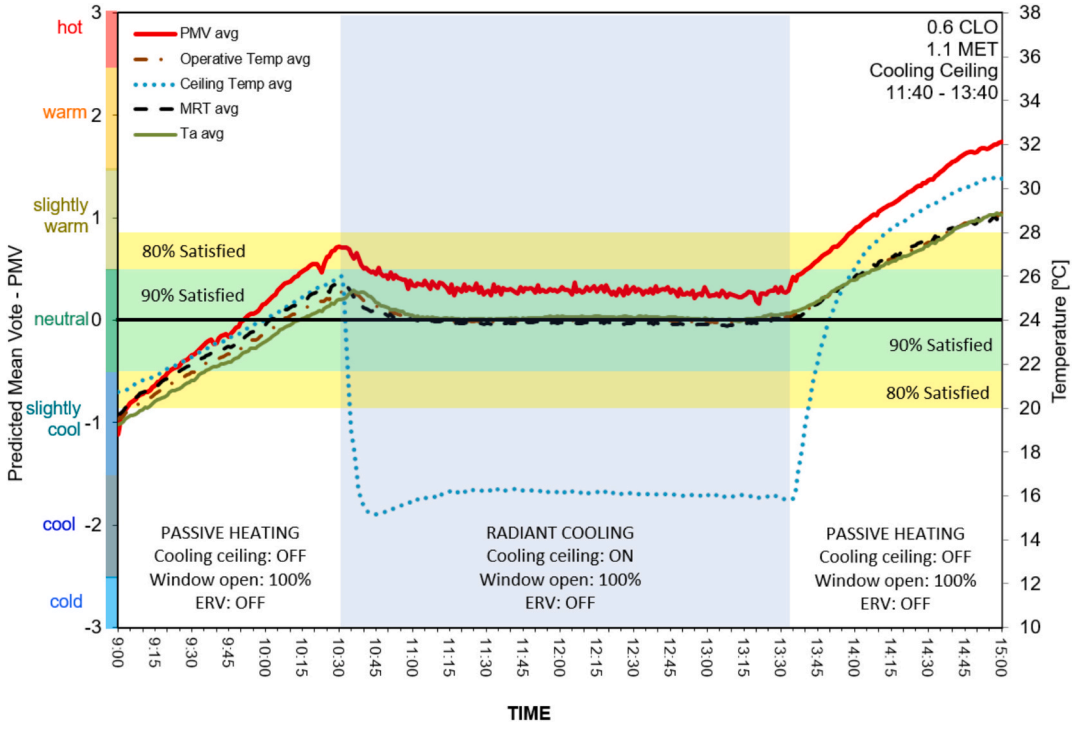

Fig. 9. Test 2 (Cooling) – Thermal Comfort, Ceiling Temperatures, MRT, and Operative Temperatures.

the PMV climbing from 0.3 (neutral) to 1.8 (warm) and out of the acceptable thermal comfort zone.

Prior to the ceiling being activated, during the first passive heating stage, the average MRT (T_r) is about 0.8 °C higher than the average air temperature (T_a). This can be explained by the effect of the heated window and solar radiation. But as the cooling ceiling is activated, the MRT (T_r) is slightly lower than the average air temperature (T_a), indicating the radiant cooling effect.

Stratification

Fig. 10 shows the air temperature (T_a) stratification within the Test-Cell. In the beginning, there is a rather uniform thermal environment within the Test-Cell. The air temperatures (T_a) between 0.1 m (near the floor) to 1.5 m (standing head high), recorded by the two comfort carts, are relatively close to each other, ranging from 19 °C to 19.8 °C. As the

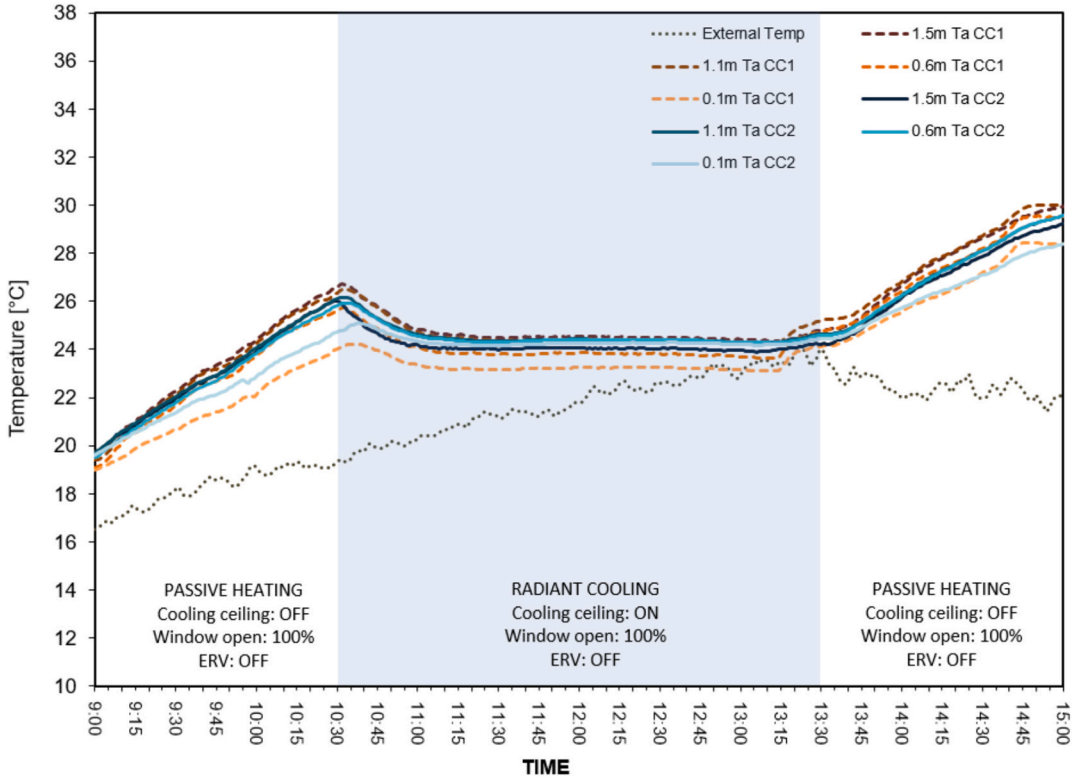

Fig. 10. Test 2 (Cooling) – Temperature Stratification.

window is fully opened and solar gain is introduced, the air temperatures (T_a) quickly increase. The readings from comfort cart 1 show that the air temperature (T_a) at 1.5 m and 1.1 m high near the window saw the fastest increase of about 7 °C in 1.5 h. Similar results are also recorded by Comfort Cart 2 near the back wall. At the same time, significant air temperature (T_a) stratifications are recorded by both comfort carts, especially near the window. The air temperature (T_a) difference between 1.5 m high (standing head high) and 0.1 m (near the floor) increases from 0.5 °C to about 2.5 °C during this passive heating stage.

As the cooling session commences, the air temperatures across the Test-Cell drop notably, indicating the operation of the cooling ceiling. The intense rising trend of the air temperatures recorded during the first

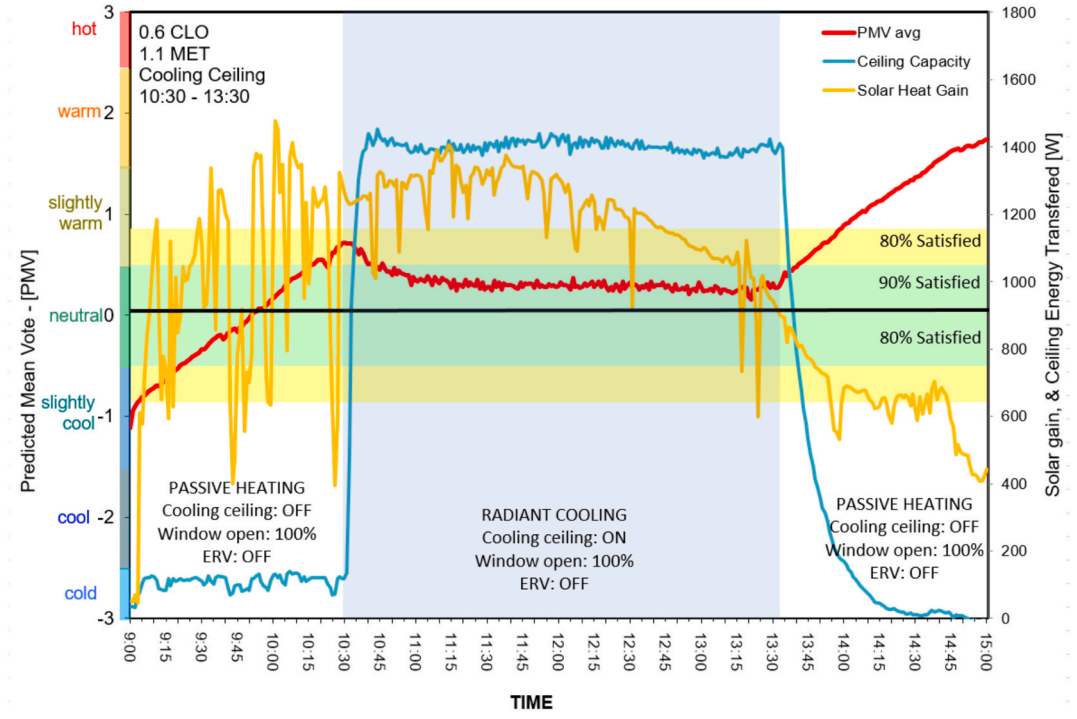

Fig. 11. Test 2 (Cooling) – Thermal comfort, solar gain, and Ceiling Capacity.

passive heating stage ceases and is replaced by a quick reduction. For example, the air temperature at 1.5 m (standing head high) and 1.1 m (sitting head high) near the window was reduced by about 2.3 °C from about 27.8 °C down to about 24.5 °C. A similar reduction is also recorded by the comfort cart 2 near the back wall at a height of 1.5 m (standing head high). The temperature gradient between 1.5 m (standing head high) and 0.1 m (near floor) is also reduced across the Test-Cell. Near the window, such temperature stratification was reduced to 1.5 °C and only 0.5 °C near the back wall. This indicates the cooling ceiling is having a convective effect and suggests that the addition of extra cooling capacity near the window could potentially improve thermal comfort.

As the cooling ceiling is deactivated, the Test-Cell is heated up passively for the second time. Here, the Test-Cell reacts similarly to the first passive heating stage. The air temperatures across the Test-Cell resume their initial rising trend, and the air stratification between different highs also increases. Before and during the measurement, the external temperature rises from about 16.5 °C to about 24 °C. From about 13:30 till the end of the measurement, the external air temperature reduces to about 22 °C.

Thermal comfort, solar gain, and ceiling capacity.

Fig. 11 shows the effect of solar heat gain and the cooling ceiling on the thermal condition within the Test-Cell. The high values of the solar heat gain are indicative of a clear and sunny day in Victoria. In the first passive heating period, the intense solar heat gain quickly affects the Test-Cell interior and increases the thermal comfort level (PMV). Despite the fluctuation, the average heat gain during this passive heating stage is about 1000 W in total. During the cooling operation, the heat gain is stable and averages at a total of 1200 W. To combat this amount of solar heat gain, the ceiling outputs a consistent 1400 W of cooling. The result is a stable thermal comfort level during the cooling session. As the cooling session concludes, the PMV rises to 1.7 (Warm) before the end of the measurements. Meanwhile, the solar heat gain keeps reducing as the sun goes down. The average solar heat gain during this second passive heating stage is about 660 W in total.

Ceiling thermal performance.

Fig. 12 shows the operational parameters of the cooling ceiling, including the heat flux (q), ceiling surface temperature (T_s), inlet water temperature (T_w), and Test-Cell operative temperature (T_o). Overall, during the cooling operation, the ceiling performed well, yielding a high heat flux (q) that reached about 90 W/m^2 average and remained stable during the cooling session. This is the result of a stable inlet water temperature (T_w) of about 12.5 °C. The average ceiling temperature (T_s) is about 16 °C, only about 3.5 °C higher than the inlet water temperature. Meanwhile, the operative temperature of the Test-Cell interior is stable at about 24 °C. Applying the readings to Eq. 3, the average total heat transfer coefficient (h_t) is about 10.5 W/m^{2}K. The ceiling also shows its fast reaction and stable operation.

3.3. Radiant cooling ceiling with external shading and heat-recovering ventilation (Test 3)

In Test 3, half of the window is covered (by the sliding gate), hence the window area that receives direct solar radiation is reduced to 3.75 m^2. The energy-recovering ventilation system is on, supplying about 150 m^3/hr of pre-conditioned fresh air. As the volume of the test cell is about 51.8 m^3, it is calculated that the ERV applies three air changes per hour, meeting the requirement for ventilation for four people in a general office space. Here, the fresh air supply for an occupant in an office space is 10L/s (36 m^3/hr) according to the Australian standard AS 1668.2:2012 for ventilation.

Thermal comfort and ceiling operation

Fig. 13 shows the result of the Test-3 cooling session. In the first stage of the test run, the room is set for passive heating with 3.75 m^2 of open window and the ERV on. In this stage, the average ceiling temperature (T_s), air temperature (T_a), MRT (T_r), and operative temperature (T_o) are similar, at about 19 °C. Here, the MRT (T_r) at the beginning of the measurements is about 0.8 °C higher than the air temperature (T_a). In about 2.5 h, the temperatures (T_a, T_o, T_r), along with the ceiling temperature within the Test-Cell, rose 8 °C to about 27 °C. Following the same trend, the average ceiling temperature (T_s) increased to about 26 °C. As a result, the PMV moved from −1.1 (slightly cool) to 1.1 (slightly warm). As the temperature increases and the PMV moves out of the 80 % satisfied comfort zone, the radiant cooling system is activated, thus starting the second stage of Test 3.

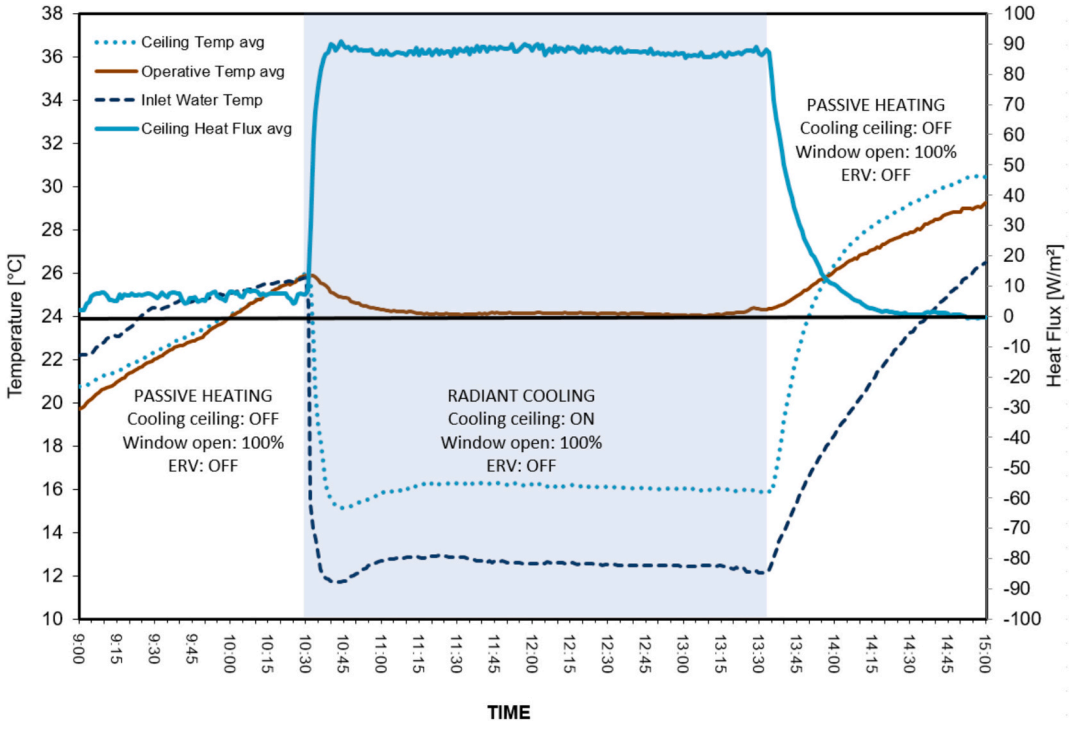

Fig. 12. Test 2 (Cooling) – Ceiling Thermal Performance.

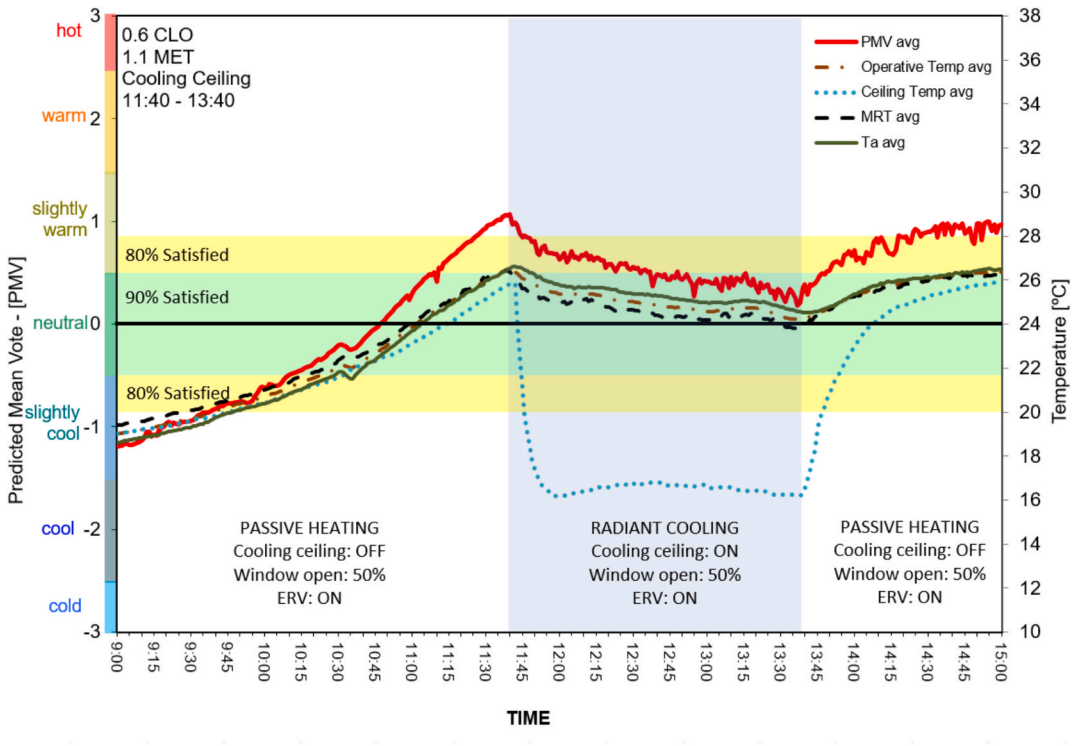

Fig. 13. Test 3 (Cooling) – Thermal Comfort, Ceiling Temperatures, MRT, and Operative Temperatures.

In the second stage, as the radiant system is turned on, the average temperature of the ceiling (T_s) drops 10 °C from about 26 °C down to 16 °C in about 15 min and stabilizes at 16.5 °C until the ceiling is turned off. The result of the cooling ceiling operation is a decrease in the operative temperature (T_o), MRT (T_r), and air temperature (T_a), as well as the PMV, indicating a return to optimal thermal comfort levels (0 – neutral) across the test cell (comfort carts 1 and 2). Interestingly, the MRT (T_r) in this stage is about 1 °C lower than the air temperature (T_a), indicating a radiant cooling effect. As the system successfully brings the PMV back to near 0 (neutral), the radiant system is turned off.

After the radiant ceiling is turned off and left to "cool down" on its own, within half an hour, the ceiling temperature (T_s) sharply increases

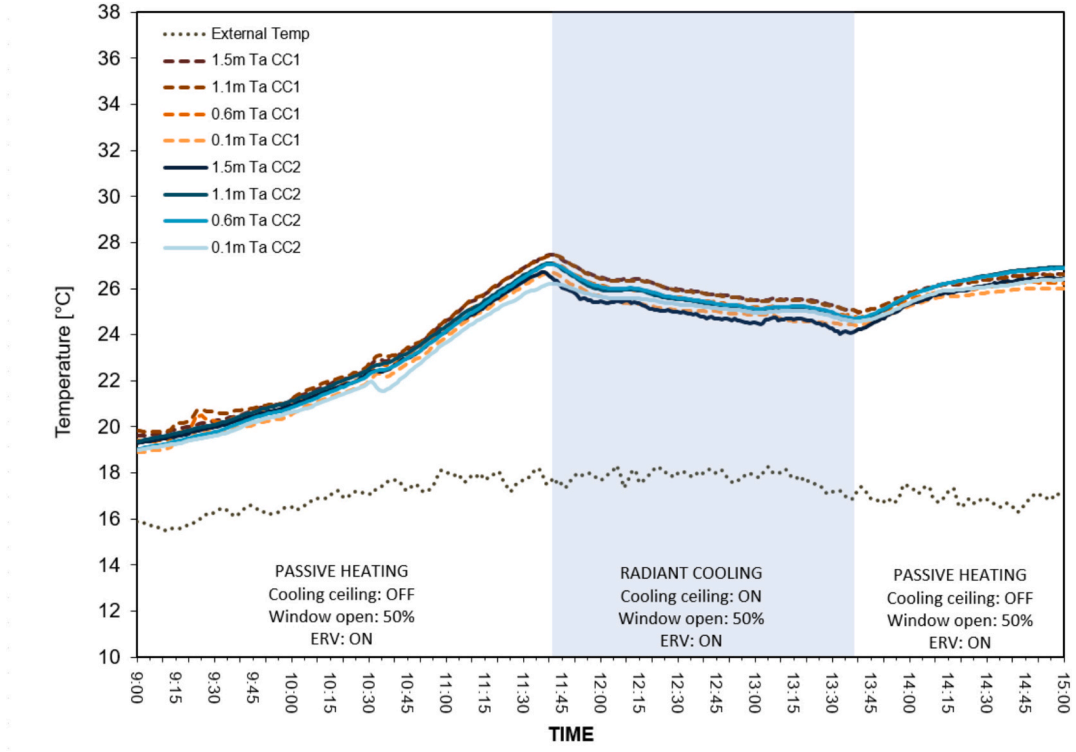

Fig. 14. Test 3 (Cooling) – Temperature Stratification.

to closely follow the operative (T_o) and MRT (T_r). Meanwhile, the Test-Cell temperatures (T_a, T_o, T_r) increased to about 26.5 °C. As a result, the PMV is about 0.8 (slightly warm) and almost out of the acceptable area.

Stratification

Fig. 14 shows the readings of room air temperature stratification (T_a) recorded by the two comfort carts (CC1 and CC2). Overall, the air readings at different heights of both comfort carts are relatively close to each other, indicating a uniform thermal environment within the Test-Cell throughout the measurement. In the first stage, the Test-Cell is passively heated up with solar radiation, hence the steady rise in air temperature (T_a). At 11:45, the radiant cooling is activated, and almost in an instant, the rising trend of the room temperature ceased and was replaced by a slow reduction. After the cooling ceiling is deactivated, the room temperature rises, and the temperature difference between the MRT (T_r) and the air (T_a) temperature is reduced. Meanwhile, the external temperature is stable, ranging between 16 and 17 °C throughout the measurement. Note that the uniformity of the air temperature is maintained before, during, and after the cooling session.

Thermal comfort, solar gain, and ceiling capacity.

Fig. 15 illustrates the effect of the external solar heat gain and the ceiling energy transfer on the Test-Cell thermal environment. Here, the total energy transfer across the 18 m^2 cooling ceiling has to combat the solar heat gain through the 3.75 m^2 window opening to condition the Test-cell. In the first Passive Heating stage, the thermal condition within the Test-Cell is dictated by the solar heat gain, which is about 600 W on average, resulting in a rapid rise in PMV. As the cooling session starts, the energy transfer between the ceiling and the Test-Cell interior sharply climbs to about 1500 W. During the cooling session, the average heat transfer of the ceiling is about 1400 W while the average solar heat is about 900 W. Hence, the cooling ceiling can successfully combat the solar heat gain and reduce the PMV from about 1 (warm) down to near 0 (neutral). After the ceiling is deactivated, the solar heat gain of 500 W average heats up the Test-Cell again.

Ceiling thermal performance.

Fig. 16 shows the thermal performance of the cooling ceiling. During the cooling session, the ceiling yields a high heat flux (q) of about 90 W/m^2 on average. In particular, the heat flux (q) reaches about 95 W/m^2 and goes down to 80 W/m^2 at the end of the session. During the stable stage of the cooling session, the inlet water temperature (T_w) is at about 12.5 °C. Here, the average ceiling temperature is 4 °C higher than the inlet water temperature (T_w) and stable at around 16.5 °C. Meanwhile, the operative temperature (T_o) reduces from 26.8 to 24 °C. Using Eq. 3, the average calculated total heat transfer coefficient (h_t) is about 10.7 W/m^2K. Such a result is similar to that of Test 2, indicating the stable operation of the system.

4. Discussion

4.1. A responsive and thermally effective system

In all of the conducted test runs, the lightweight and modular ceiling system proved to be highly responsive and thermally effective. In particular, the ceiling shows its capacity for providing and maintaining appropriate levels of thermal comfort in both heating and cooling scenarios. In all of the test runs, the ceiling is also proven to be highly responsive. In the cooling sessions, as the ceiling is activated and conditioned water is pumped throughout, the ceiling reaches its full capacity in terms of heat flux or surface temperature in around 15 min. In the heating test run, despite the heat pump's fluctuating operation, the ceiling shows its fast reaction, as the ceiling surface temperature closely follows the fluctuation of the inlet water temperature. In all of the test runs, the difference between the inlet water temperature and the average radiant ceiling surface temperature remains within the range of 3.5 to 4 °C. Details are shown in Table 4 below.

The low temperature difference between the inlet water and the ceiling surface indicates a low heat transfer resistance between the radiant surface and the water within the panels, implying a thermally effective system. As a result, as the ceiling is activated, the thermal effect is almost instantaneous, with dynamic changes in thermal conditions recorded, particularly notable in cooling mode. As mentioned in section 2.3, the metal panels are expected to have lower thermal resistance than the plasterboard panels. The results shown in Table 4 indicate that this is the case.

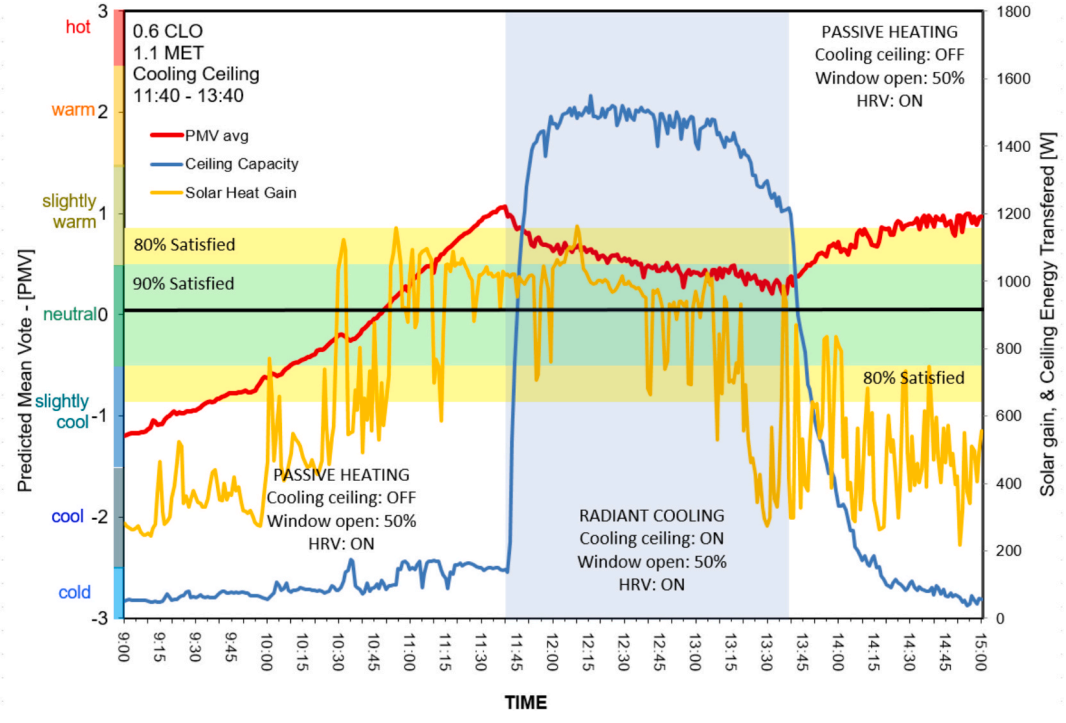

Fig. 15. Test 3 (Cooling) – Thermal comfort, solar gain, and ceiling capacity.

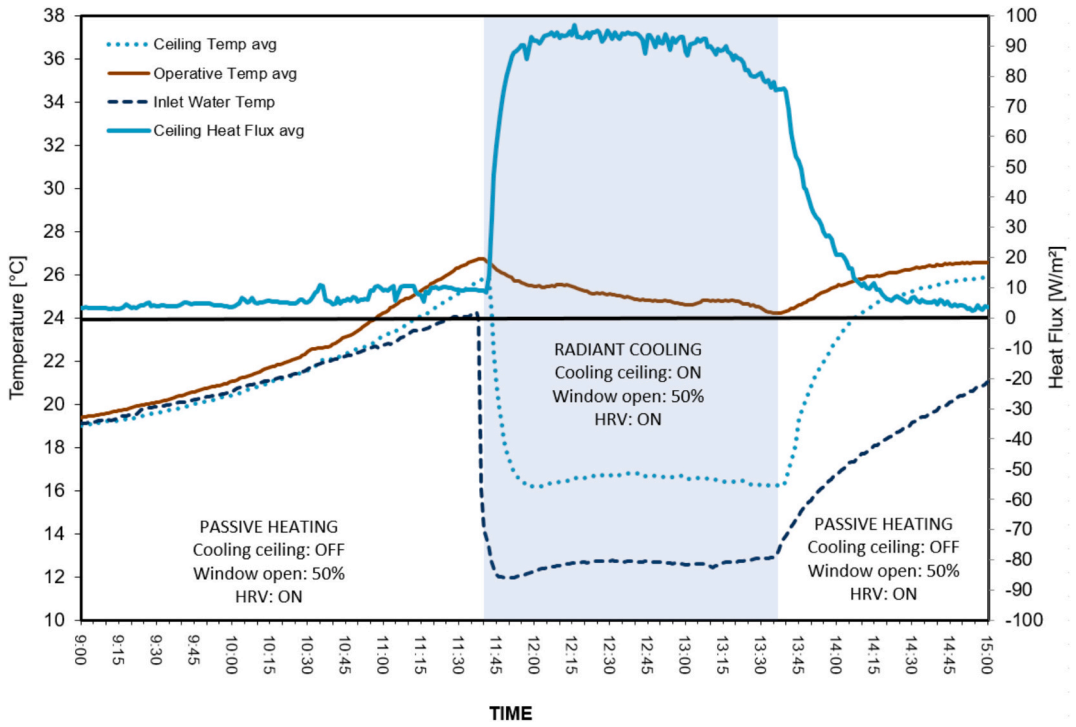

Fig. 16. Test 3 (Cooling) – Ceiling thermal performance.

Table 4
Temperature difference between the inlet water and the ceiling surface.

Temperature Difference between the Inlet Water and the Ceiling Surface	Test 1Heating Ceiling	Test 2Cooling Ceiling	Test 3Cooling Ceiling
Metal panels	2.9 °C	3.1 °C	3.5 °C
Plaster panels	4.3 °C	4.1 °C	4.5 °C
Average	3.6 °C	3.5 °C	4 °C

4.2. Challenges for radiant heating ceiling

Test run 1 confirms the effectiveness of the heating ceiling. While the heating ceiling achieved the 'optimal' level of thermal comfort, it did take over an hour for the PMV to rise from −2 up to an acceptable level of −0.8. Such a delayed effect indicates that the radiant heating ceiling, although responsive, may not be optimally effective when encountering dynamic thermal conditions.

The average ceiling heat flux (q) is 85 W/m^2 during heating, while the temperature difference between the radiant ceiling surface and the operative temperature (T_o) is high at about 13.5 °C. The result gives a total heat transfer coefficient (h_t) of about 6.3 W/m^{2}K for the whole ceiling, on average. While this result is similar to those provided in the REHVA handbook and other publications [28], this low heat transfer coefficient severely limits the heating ceiling's conditioning capacity. This is particularly true given the very small convective component of radiant heating ceilings, with radiant heat transfer accounting for approximately 5.5 W/m^{2}K [28] within a 6.3 W/m^{2}K total heat transfer coefficient (h_t).

A further problem noted is the high vertical air temperature stratification that occurs during the heating session. As the heating ceiling is activated, the vertical air temperature gradient increases over time. After three hours, the air temperature (T_a) difference between the standing head height (1.5 m) and the foot height (0.1 m) can reach nearly 3 °C. Such a temperature gradient reveals a likelihood of local thermal discomfort. In comparison, in "Case 3" of the experiment conducted by Zhao *et al.* [14], when 39.7 °C (similar to the 40 °C of Test1) water is supplied to their heating ceiling, the air temperature difference between the 1.5 m and 0.1 m is only 2 °C.

However, when a convective aid (ERV) is provided in Test 3, a uniform thermal condition is created. This result suggests that if convection aid (air movement) is provided to mix the air and reduce temperature stratification, the thermal comfort performance of the heating ceiling will be significantly enhanced. Additionally, convection aid (air movement) can also improve convective heat transfer for the radiant ceiling [9], which is highly useful for improving the heat flux output for the heating ceiling.

4.3. Positive results for radiant cooling at perimeter zones

The two cooling sessions show the capacity of a radiant cooling ceiling system to achieve and maintain appropriate levels of thermal comfort. Even on a hot summer day, with a window-to-wall ratio of 70 %, and without the additional convective aid (Test 2), the cooling ceiling successfully yields about 90 W/m^2 to 95 W/m^2 heat flux (q), providing and maintaining an acceptable level of thermal comfort. In the two cooling test runs, the system also performs consistently in terms of water temperature (T_w), ceiling surface temperature (T_s), and heat flux output (q).

Moreover, in both cooling test runs, the total heat transfer coefficient (h_t) results are similar, at 10.5 W/m^{2}K for Test 2, and 10.7 W/m^{2}K for Test 3. These results are close to the total heat transfer coefficient proposed by the REHVA handbook (11 W/m^{2}K) and the EN1264-5 standard (10.8 W/m^{2}K), and higher than the results of several previous publications [28]. Such a high total heat transfer coefficient (h_t) value was achieved due to efficient convective heat transfer (h_c), 5 W/m^{2}K for Test 2 and 5.2 W/m^2 for Test 3. Note, in Test 2, the cooling radiant ceiling is operated without mechanical ventilation, while in Test 3, the ERV is activated, providing additional convection. Such results indicate that in Test 2, the cooling ceiling alone can promote appropriate air movement to generate adequate convective heat transfer.

However, the benefit of having additional convective aid is shown when comparing the air temperature (T_a) stratification between the two cooling tests. In Test 3, with the additional air movement added by the

ERV, the vertical air temperature stratification is much lower than that of Test 2. Also in Test 2, the reason the cooling ceiling manages to maintain an acceptable level of thermal comfort is due to the fact that the ceiling is activated before the PMV moves out of the comfort zone (−0.8 to 0.8).

4.4. MRT, operative temperature, and air temperature

In all three experiments, the average MRT (*MRT* avg), average operative temperature (T_o avg), and average air temperature (T_a avg) follow each other closely. The temperature difference between MRT and air temperature is consistently less than 1 °C, with less than 0.5 °C between the operative temperature and air temperature. When the radiant ceiling is activated, the MRT, operative temperature, and air temperature are affected, with little time lag noted. This indicates the high impact of radiant conditioning not just on MRT, but also on the air temperature (and operative temperature as a derivative of the two). This corresponds with the findings of Jia *et al.* [6] in their experiment with radiant systems in a perimeter office space, where the authors recorded less than a 0.7 °C difference between the operative temperature and air temperature.

While all test runs (heating and cooling) record a close correspondence between temperatures (T_r, T_o, T_a), the change in MRT (T_r) is more notable in the cooling tests. Here, in the first passive heating stage of both cooling test runs, the average MRT (T_r) is higher than the average air temperature (T_a). This can be attributed to the solar radiation and the consequent heated window. But when the cooling ceiling is activated, the average MRT (T_r) rapidly drops lower than the average air temperature (T_a). This is most notable in Test 3, when the cooling ceiling is activated, the average MRT (T_r) is approximately 1 °C lower than the air temperature (T_a).

Nevertheless, the significant conditioning effect of the radiant ceiling on the air temperature (T_a) is noted and reinforces the suggestion that the average air temperature may be appropriately used to control such a radiant system [6]. The air temperature (T_a) can be easily monitored using existing and readily accessible thermal sensors, so this approach has significant benefits. Additionally, in Test 3, when supplementary ventilation is applied, a uniform thermal environment is recorded in the Test-Cell, making air temperature control for the radiant ceiling even more viable.

4.5. Extra conditioning capacity near the window

Fig. 17 shows that the lighter metal radiant ceiling panels are thermally superior to their plasterboard counterparts. The metal panels near the window yield a 10 % higher heat flux (q) in both heating and cooling. Hence, deploying the metal panels near the window successfully provides extra conditioning capacity.

Also shown in Fig. 17 is the MRT (T_r) recorded by the thermal comfort carts in the three test runs. In Test 1 with the heating ceiling, the MRT (T_r) near the window (CC1) is slightly lower than that recorded further back (CC2). This difference is an indication of the heat loss through the window. Similarly, in the two cooling test runs, the MRT (T_r) near the window is slightly higher, due to the window being heated by direct solar radiation. As the ceiling is activated, the difference between the MRT (T_r) recorded by CC1 and CC2 remains stable in all tests. Hence, it can be concluded that the benefit of having separate premium panels to provide extra capacity near the window is marginal.

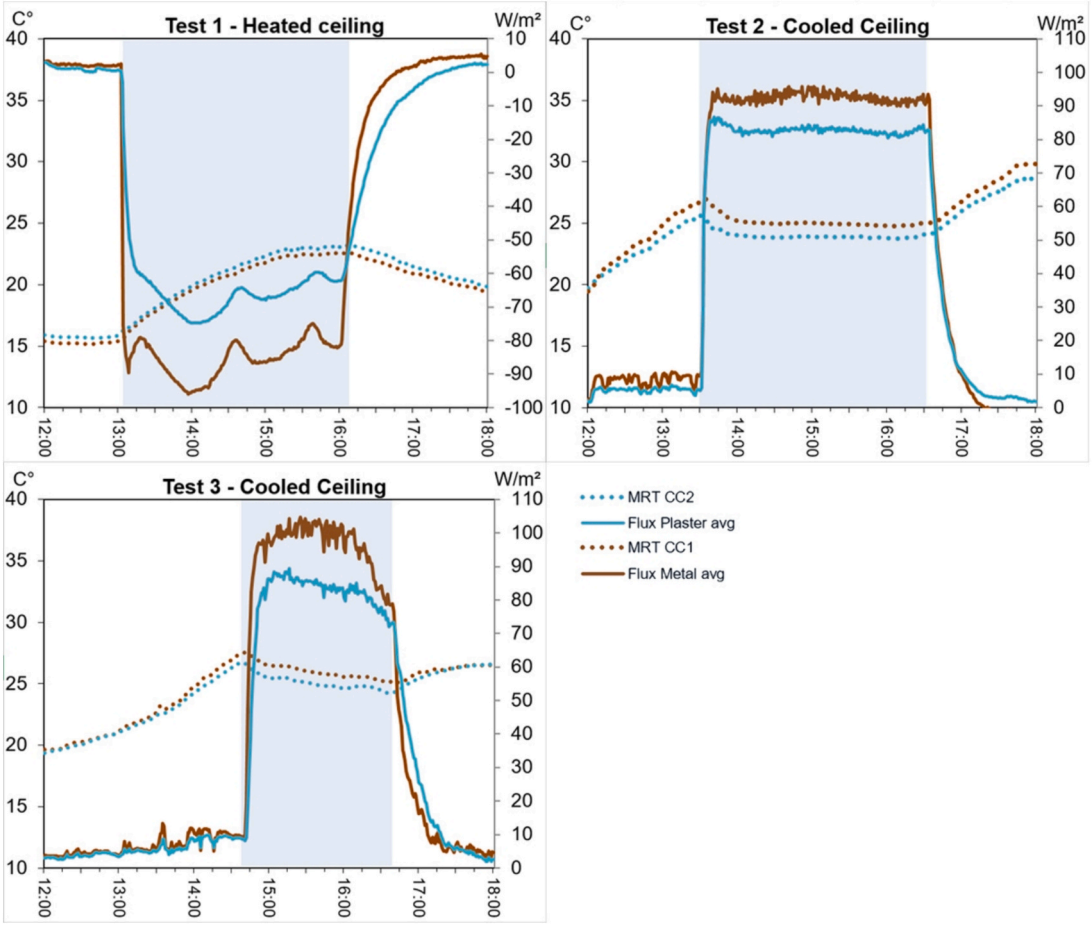

Fig. 17. Ceiling panel heat flux and MRT.

However, when examining the air stratification in Test 2, the extra cooling capacity near the window can be seen to help reduce the vertical stratification recorded by CC1 (Fig. 10). Prior to the cooling ceiling activation, the vertical air temperature (T_a) gradient near the window increased dramatically in response to solar gain. Once the ceiling was activated, the stratification reduced significantly, indicating a benefit of having separated premium panels near the window. Yet, in Test 3, the addition of the ventilation system overrides this benefit.

5. Conclusion

5.1. Conclusion

In this study, three instrumental experiments are conducted for both heating and cooling with respect to radiant conditioning. The experiments were carried out in a dedicated, fully instrumented test chamber, built in compliance with the Australian Construction Code, modeling a north-facing perimeter office room. Based on the results and discussion, the conclusions of this study are as follows:

- In this study, a lightweight and modular radiant ceiling system is introduced. Through instrumental experiments, the radiant ceiling is proven to be highly responsive and thermally effective. The radiant ceiling is capable of yielding a high heat flux of 85 W/m^2 in heating, and 90–95 W/m^2 in cooling. Upon activation, the ceiling reaches its stable state in approximately 15 min.
- The lightweight and radiant ceiling system is capable of providing and maintaining thermal comfort both in heating and cooling. In heating mode, the radiant ceiling successfully increased PMV from “cool” to “neutral”. In cooling mode, even when operating alone against the heavy solar heat gain of a north-facing perimeter room, the ceiling is still capable of maintaining an acceptable level of thermal comfort.
- Although it is feasible to achieve thermal comfort with a heating radiant ceiling without additional convection, there is a risk of high vertical temperature stratification, leading to local thermal discomfort. Therefore, suitable assisted mechanical ventilation is recommended in order to mix the air and mitigate the high vertical air temperature gradient of the radiant heating ceiling. In a further anticipated study, a ceiling fan will be introduced and tested in the heating ceiling.
- At perimeter zones, the radiant cooling ceiling can promote air movement and achieve a high convective heat transfer coefficient without additional convection. However, mechanical convective aid is recommended in order to generate a more uniform air temperature and a consequent conducive thermal environment.
- In all three experiments, the conditioning effect of the radiant system is equally significant on air temperature as it is on MRT. The highest recorded difference between the air temperature and MRT is merely 1 °C, recorded in Test 3. Hence, air temperature may be effectively used to control the radiant system.

This research focuses specifically on the conditioning of the proposed radiant ceiling. It is well established that air movement can enhance heat transfer between radiant systems and the conditioned environment. Yet, having additional mechanical ventilation can also mitigate some limitations of radiant conditioning while creating a more uniform thermal environment. Nevertheless, radiant systems cannot in themselves provide fresh air and must always work in conjunction with HVAC systems. How these two systems should be combined for maximum efficiency warrants further investigation. Experimental focus on air movement as well as humidity control will be explored in future research.

In terms of practical application, the combination of radiant and convective systems is highly promising for combating heat gain in perimeter zones. This system can run efficiently using water at 12 °C. This water temperature can easily be accommodated through an existing chilled water system supplied in commercial office buildings. Indeed, the return water from an AHU could facilitate this task easily, thus circumventing the requirement for additional cooling capacity with an HVAC system.

5.2. Limitations and future research

While the system tested was capable of heating and providing thermal comfort (Test 1), it is also evident that the heat pump was unstable during heating. The limited heating capacity of the heat pump resulted in a maximum water temperature of 42 °C. This, coupled with a hot water storage tank capacity of 100L, was not enough to stabilize the inlet water temperature, resulting in a fluctuation of approximately 2 °C in heating inlet water temperature during Test 1. While this fluctuation range was not sufficient to cause any notable impact on the PMV, air temperature, or mean radiant temperature, such fluctuations are not ideal for prolonged operation. A high-capacity heat pump and a 1000 L hot water storage tank are being sourced for future experiments.

Additionally, while several tests were conducted to calibrate the system and check its functionality, the results presented in this paper are based on two cooling test runs and a single heating run. While the results of this study are generally in alignment with the results of several previous studies, ideally, at least three test runs should be conducted for each case to allow for broader generalizability of the results. With a new heat pump and an improved storage tank, further experiments will be conducted to reinforce the results of this study.

Credit authorship contribution statement

Hung Q. Do: . **Mark B. Luther:** Writing – review & editing, Supervision, Resources, Methodology, Conceptualization. **Jane Matthews:** Writing – review & editing, Supervision, Methodology, Formal analysis, Conceptualization. **Igor Martek:** Writing – review & editing, Supervision.

Declaration of competing interest

The authors declare that they have no known competing financial interests or personal relationships that could have appeared to influence the work reported in this paper.

Data availability

Data will be made available on request.

References

[1] M. Shin, J.S. Haberl, Thermal zoning for building HVAC design and energy simulation: a literature review, Energ. Buildings 203 (2019) 109429.
[2] M. Bessoudo, et al., Indoor thermal environmental conditions near glazed facades with shading devices–Part I: Experiments and building thermal model, Build. Environ. 45 (11) (2010) 2506–2516.
[3] P. Mustakallio, et al., Thermal environment in simulated offices with convective and radiant cooling systems under cooling (summer) mode of operation, Build. Environ. 100 (2016) 82–91.
[4] P. Mustakallio, et al., Thermal environment in a simulated double office room with convective and radiant cooling systems, Build. Environ. 123 (2017) 88–100.
[5] T. Catalina, J. Virgone, F. Kuznik, Evaluation of thermal comfort using combined CFD and experimentation study in a test room equipped with a cooling ceiling, Build. Environ. 44 (8) (2009) 1740–1750.
[6] H. Jia, X. Pang, P. Haves, Experimentally-determined characteristics of radiant systems for office buildings, Appl. Energy 221 (2018) 41–54.
[7] J.D. Feng, S. Schiavon, F. Bauman, Cooling load differences between radiant and air systems, Energ. Buildings 65 (2013) 310–321.
[8] A. Moftakhari, S. Bourne, A. Novoselac, Cooling load comparison of rooms conditioned with radiant cooling panels and all-air HVAC systems (ASHRAE RP 1729), Sci. Technol. Built Environ. 29 (3) (2023) 280–296.
[9] L. Zhang, X.-H. Liu, Y. Jiang, Experimental evaluation of a suspended metal ceiling radiant panel with inclined fins, Energ. Buildings 62 (2013) 522–529.

[10] L. Ding, et al., Thermal performance analyses of a new multi-segmented minichannel-based radiant ceiling cooling panel, Energy Rep. 6 (2020) 1409–1415.
[11] J. Du, et al., A numerical study on the effects of design/operating parameters of the radiant panel in a radiation-based task air conditioning system on indoor thermal comfort and energy saving for a sleeping environment, Energ. Buildings 151 (2017) 250–262.
[12] J. Miriel, L. Serres, A. Trombe, Radiant ceiling panel heating–cooling systems: experimental and simulated study of the performances, thermal comfort and energy consumptions, Appl. Therm. Eng. 22 (16) (2002) 1861–1873.
[13] A.A. Serageldin, et al., Numerical investigation of the thermal performance of a radiant ceiling cooling panel with segmented concave surfaces, J. Build. Eng. 42 (2021) 102450.
[14] M. Zhao, et al., Experimental investigation and feasibility analysis on a capillary radiant heating system based on solar and air source heat pump dual heat source, Appl. Energy 185 (2017) 2094–2105.
[15] J. Joe, P. Karava, A model predictive control strategy to optimize the performance of radiant floor heating and cooling systems in office buildings, Appl. Energy 245 (2019) 65–77.
[16] H.Q. Do, et al., Development and thermal performance testing of radiant conditioning ceiling panels, Archit. Sci. Rev. (2024) 1–12.
[17] M. Mosa, M. Labat, S. Lorente, Constructal design of flow channels for radiant cooling panels, Int. J. Therm. Sci. 145 (2019) 106052.
[18] H.Q. Do, et al., Optimizing Conditioning Systems in the Perimeter Zones of Office Buildings, Architectural Science Association, 2022.
[19] Babiak, J., B.W. Olesen, and D. Petras, Low temperature heating and high temperature cooling: REHVA GUIDEBOOK No 7. 2007.
[20] H.Q. Do, et al., An experimental evaluation of the thermal performance of lightweight radiant ceiling panel designs, Energ. Buildings (2025) 115966.
[21] Z. Jing, L. Jiayu, Study on heat transfer delay of exposed capillary ceiling radiant panels (E-CCRP) system based on CFD method, Build. Environ. 180 (2020) 106982.
[22] P. Ding, et al., Study on heating capacity and heat loss of capillary radiant floor heating systems, Appl. Therm. Eng. 165 (2020) 114618.
[23] D. Xing, N. Li, Reconstruction of hydronic radiant cooling panels: Conceptual design and numerical simulation, Therm. Sci. Eng. Prog. 30 (2022) 101272.
[24] R. De Dear, G.S. Brager, The adaptive model of thermal comfort and energy conservation in the built environment, Int. J. Biometeorol. 45 (2) (2001) 100–108.
[25] M. Luther, O. Tokede, C. Liu, Applying a comfort model to building performance analysis, Archit. Sci. Rev. 63 (6) (2020) 481–493.
[26] ASHRAE, ASHRAE Standard 55-2017: Thermal environment conditions for human occupancy. 2017, Atlanta, GA: American Society of Heating, Refrigerating and Air Conditioning Engineers Inc.
[27] R.J. de Dear, et al., Progress in thermal comfort research over the last twenty years, Indoor Air 23 (6) (2013) 442–461.
[28] J. Shinoda, et al., A review of the surface heat transfer coefficients of radiant heating and cooling systems, Build. Environ. 159 (2019) 106156.